RESEARCH ARTICLE | DECEMBER 20 2021

PT symmetric dynamics in counter-rotating gyroscopic mechanical systems

Bin Dong ; Chengzhi Shi ; Robert G. Parker

AIP Advances 11, 125224 (2021)
https://doi.org/10.1063/5.0073859

PT symmetric dynamics in counter-rotating gyroscopic mechanical systems

Cite as: AIP Advances **11**, 125224 (2021); doi: 10.1063/5.0073859
Submitted: 7 October 2021 • Accepted: 29 November 2021 •
Published Online: 20 December 2021

Bin Dong,[1] Chengzhi Shi,[2,a)] and Robert G. Parker[1]

AFFILIATIONS

[1] Department of Mechanical Engineering, University of Utah, Salt Lake City, Utah 84102, USA
[2] George W. Woodruff School of Mechanical Engineering, Georgia Institute of Technology, Atlanta, Georgia 30332, USA

[a)] Author to whom correspondence should be addressed: chengzhi.shi@me.gatech.edu

ABSTRACT

Parity-time (PT) symmetry was first studied in quantum mechanical systems with a non-Hermitian Hamiltonian whose observables are real-valued. Most existing designs of PT symmetric systems in electronics, optics, and acoustics rely on an exact balance of loss and gain in the media to achieve PT symmetry. However, the dispersive behavior of most loss and gain materials restricts the frequency range where the system is PT symmetric. This makes it challenging to access the exceptional points of the system to observe the PT symmetric transition dynamics. Here, we propose a new path to realize PT symmetric systems based on gyroscopic effects instead of using loss and gain units. We demonstrate that PT symmetry and the occurrence of exceptional points are preserved for inversive, counter-rotating gyroscopic systems even with dispersive sub-units. In a gyroscopic system with two circular rings rotating in opposite directions at the same speed, the spontaneous symmetry breaking across the exceptional points results in a phase transition from a moving maximum deformation location to a motionless maximum point. The motionless maximum point occurs despite the externally imposed rotation of the two rings. The results set the foundation to study nonlinear dispersive physics in PT symmetric systems, including solitary waves and inelastic wave scattering.

Parity-time (PT) symmetric systems are invariant under the combined parity and time reversal operation. A non-Hermitian system with PT symmetry can exhibit an entirely real-valued spectrum while complex-valued eigenvalues appear as a result of parameter variations that lead to a phase transition in the system.[1–3] The symmetry-breaking thresholds in the parameter space at which two or more eigenvalues become degenerate are known as the exceptional points of PT symmetric systems. At the exceptional points, the Hamiltonian transitions from the PT-exact phase to the PT-broken phase or vice versa.[2,4,5] The PT-exact phase consists of the parameter space where the system spectrum is real-valued, while the PT-broken phase marks the parameter space where the spectrum contains complex-valued eigenvalues. The eigenvector, or the subspace spanned by the eigenvectors, associated with any eigenvalue is invariant under PT symmetry in a PT-exact phase but is not in a PT-broken phase. Various concepts related to PT symmetry, including anti-PT symmetry, are widely explored in electronics,[6,7] heat and mass transfer,[8] optics,[4,9–13] and acoustics.[14–18] Many intriguing phenomena are related to phase transitions of the system Hamiltonians that occur at the exceptional points. Accessing the exceptional points enables ultrasensitive measurements,[19–21] manipulation of the modal content of multimode lasers,[22–25] and realization of asymmetric wave transport in both optics and acoustics.[10,26–29]

Most studies rely on an exact loss and gain balance in the medium to achieve PT symmetry of a system, but the dispersive behavior of most loss and gain materials prevents achieving this condition over a broad frequency range. Obtaining the exceptional points of these dispersive systems requires judicious tuning of the gap size between the loss and gain media.[16] However, this approach changes the physical configuration of the system and the corresponding Hamiltonian. Thus, the tuning approach cannot be applied to study the phase transition dynamics around the exceptional points of a system with a given Hamiltonian. To observe the PT-phase transition dynamics of a specific Hamiltonian, it is desirable to develop a new platform of PT symmetric systems where the PT symmetry is independent of material dispersion and the exceptional points can be robustly obtained.

We propose a new path to realize systems with PT symmetric dynamics by using the gyroscopic effects in moving media.

Gyroscopic effects in mechanical systems are those arising from Coriolis accelerations. The conditions for a general gyroscopic vibratory system to be PT symmetric are derived. Based on the derived conditions, counter-rotating gyroscopic systems, defined as those where two identical coupled bodies (i.e., sub-units) rotate in opposite directions at the same speed, are PT symmetric. They can possess and operate around exceptional points by tuning the sub-unit rotation speed. Compared to designs based on the loss and gain balance, the dispersion of the materials used in the sub-units of counter-rotating gyroscopic systems neither affects the PT symmetry of the system nor prevents the occurrence of exceptional points. We investigate the dynamics of two systems consisting of counter-rotating rings (dispersive) and strings (non-dispersive) to illustrate qualitative dynamic properties of counter-rotating gyroscopic systems across the phase transition.

The equation of motion for a general gyroscopic system under free vibration is $\mathbf{M}\ddot{\boldsymbol{q}} + \mathbf{G}\dot{\mathbf{q}} + \mathbf{K}\mathbf{q} = \mathbf{0}$, where $\mathbf{M}$ is the inertia operator, $\mathbf{G} = \mathbf{C} + \Omega\hat{\mathbf{G}}$ consists of the damping ($\mathbf{C}$) and gyroscopic ($\Omega\hat{\mathbf{G}}$) operators, $\mathbf{K} = \mathbf{K}_s - \Omega^2\hat{\mathbf{K}}$ contains the stiffness ($\mathbf{K}_s$) and centripetal acceleration ($-\Omega^2\hat{\mathbf{K}}$) operators, and Ω is the rotation speed of system. $\mathbf{M}$ is independent of the rotation speed of the system. The gyroscopic operator, which arises from Coriolis accelerations, is proportional to the rotation speed. $\mathbf{K}$ includes a term that is quadratic in the rotation speed.

General gyroscopic systems do not necessarily satisfy PT symmetry. Gyroscopic effects can occur in systems without inversion symmetry of their geometry, and gyroscopic effects break the time reversal symmetry in general, i.e., $\mathbf{q}(-t)$ is not a solution of the equation of motion. As shown in the supplementary material, Note 1, the condition for a general gyroscopic system to be PT symmetric is that the operators $\mathbf{M}$ and $\mathbf{K}$ are invariant under the PT symmetry operation, i.e., $(PT\mathbf{M}(PT)^{-1} = \mathbf{M}$, while the operator $\mathbf{G}$ satisfies $(PT\mathbf{G}(PT)^{-1} = -\mathbf{G}$. For systems where $\mathbf{M}$, $\mathbf{G}$, and $\mathbf{K}$ are time independent, $\mathbf{M}$ and $\mathbf{K}$ need to be invariant under parity symmetry (i.e., $P\mathbf{M}P^{-1} = \mathbf{M}$) while $\mathbf{G}$ is anti-parity symmetric ($P\mathbf{G}P^{-1} = -\mathbf{G}$). Because $\mathbf{G}$ consists of damping ($\mathbf{C}$) and gyroscopic ($\Omega\hat{\mathbf{G}}$) operators, the condition for PT symmetry is that both $\mathbf{C}$ and $\Omega\hat{\boldsymbol{G}}$ are anti-parity symmetric.

A particular type of gyroscopic system naturally satisfies the above-mentioned conditions for being PT symmetric. A system of this type is characterized by two identical sub-units that move at the same speed Ω in opposite directions. This is referred to as a **counter-rotating gyroscopic system** in this work. For a system with two identical sub-units, application of the parity operation on a deformation $\mathbf{q}$ of the system exchanges the deformations $\mathbf{q}_1$ and $\mathbf{q}_2$ of the two sub-units, i.e., $P\mathbf{q} = P(\mathbf{q}_1, \mathbf{q}_2)^T = (\mathbf{q}_2, \mathbf{q}_1)^T$. The inertia operator $\mathbf{M}$ is independent of the sub-unit rotation speed Ω, and the centripetal acceleration of the system $-\Omega^2\hat{\mathbf{K}}$ is independent of the sign of Ω. $\mathbf{M}$ and $\mathbf{K}$ are invariant under parity symmetry because the sub-units are identical and both $\mathbf{M}$ and $\mathbf{K}$ are independent of the directions in which the sub-unit moves. In contrast, the gyroscopic operator $\Omega\hat{\mathbf{G}}$ in $\mathbf{G}$ is proportional to the rotation speed of the sub-units. Because the two sub-units move in opposite directions at the same speed, $\Omega\hat{\mathbf{G}}$ is anti-parity symmetric. Meanwhile, the damping operator $\mathbf{C}$ is also anti-parity symmetric, which indicates the two sub-units need to have the exact energy loss and gain balance to satisfy the PT symmetric condition. In this work, the operator $\mathbf{G}$ only models gyroscopic effects. Damping terms (linear loss and gain) are excluded, i.e., $\mathbf{G} = \Omega\hat{\mathbf{G}}$. Therefore, counter-rotating gyroscopic systems satisfy all the conditions of PT symmetry. Gyroscopic effects are sufficient to achieve the PT symmetry, and no loss and gain sub-units are needed.

Exceptional points occur in the parameter space of counter-rotating gyroscopic systems, specifically the parameter of rotation speed. As special cases of gyroscopic systems, counter-rotating gyroscopic systems experience instability similar to known instabilities of general gyroscopic systems. The boundaries between stable and unstable operating speeds are the exceptional points of counter-rotating gyroscopic systems. These are speeds at which two or more eigenvalues coalesce and become degenerate. These exceptional points are frequently referred to as critical speeds in mechanics literature.[30–33] The lowest exceptional point occurs when $\mathbf{K}$ ceases to be positive-definite because of the centripetal term $-\Omega^2\hat{\mathbf{K}}$. Across this exceptional point, gyroscopic systems, including counter-rotating gyroscopic systems, frequently transition from stable to unstable or vice versa as the rotation speed increases. Many gyroscopic systems, such as axially moving strings/beams and spinning disks with a transverse stiffness, recover stability with a further increase in the speed despite the stiffness operator being sign indefinite at these higher speeds.[32,33] Threshold speeds where a gyroscopic system recovers stability after a region of instability are also the exceptional points if the system is a counter-rotating gyroscopic system. The occurrence of exceptional points in counter-rotating gyroscopic systems is not related to dispersive properties of the sub-units.

The gyroscopic term in the equation of motion is a result of the Coriolis effect in rotating frames. In optics and acoustics, the Coriolis effect of frame rotation leads to the well-known optical and acoustic Hall effects.[34,35] In both classical Hall effect and spin-Hall effect, the trajectories of the current-carry particles or the propagating directions of optical and acoustic waves are under the impact of external magnetic fields, the spins of particles, and the wave polarizations. For example, changing the sign of the external magnetic field will change the sign of Hall voltage due to the classical Hall effects, and particles with spins of opposite signs are accumulated on opposing surface boundaries due to the spin-Hall effects. All these phenomena are analogous to the gyroscopic effect as discussed above: the sign of the gyroscopic operator $\Omega\hat{\boldsymbol{G}}$ changes if the system is moving in the opposite direction at the speed Ω.

These Hall effects induce many interesting physical phenomena including spin-momentum locking,[36,37] topological optics and acoustics,[38,39] and chiral quantum photonics.[40] However, the Hall effect induced PT symmetric properties and phase transition dynamics have not been observed. In this paper, we demonstrate the feasibility of PT symmetric phase transition dynamics induced by the gyroscopic effect in a pair of simple counter-rotating rings forming a gyroscopic system. Similar PT symmetric properties are expected to be induced by the Hall effects of optical and acoustic waves propagating in coupled, counter-rotating optical and acoustic waveguides.

We consider the vibration of two counter-rotating rings as shown in Fig. 1(a). The two identical rings rotate at the same speed Ω but in opposite directions. A uniformly distributed elastic foundation couples the two rings, and both rings are supported on elastic

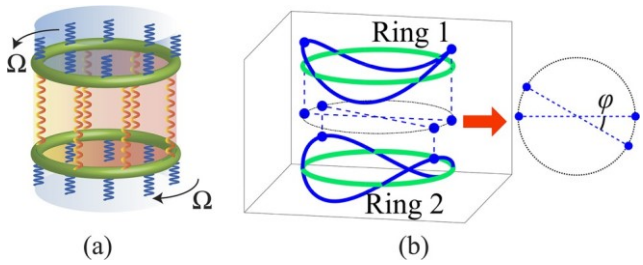

FIG. 1. (a) PT symmetric system consisting of counter-rotating rings. Two identical rings are rotating at identical speed $\boldsymbol{\Omega}$ but in opposite directions. Both rings are supported on uniformly distributed elastic foundations (springs in blue). They are coupled through a uniform elastic spring (in orange). (b) Representation of ring deformations. Ring deformations (solid lines in blue) are purely out of plane. The blue dots represent the locations of maximum deformation of the rings. $\boldsymbol{\varphi}$ denotes the angle between diameters of points of maximum deflection on the two rings.

foundations of equal stiffness that can differ from the coupling stiffness. The system is a counter-rotating gyroscopic system as defined earlier. As illustrated in Fig. 1(b), only out-of-plane deformations are allowed. The non-dimensional equations of motion are

$$\frac{\partial^2 w}{\partial t^2} + 2\Omega\frac{\partial}{\partial t}\left(\frac{\partial w}{\partial \theta}\right) + (\Omega^2 - 1)\frac{\partial^2 w}{\partial \theta^2} + \kappa\frac{\partial^4 w}{\partial \theta^4} + (\beta_1 + \beta_2)w - \beta_2 u = 0, \tag{1a}$$

$$\frac{\partial^2 u}{\partial t^2} - 2\Omega\frac{\partial}{\partial t}\left(\frac{\partial u}{\partial \theta}\right) + (\Omega^2 - 1)\frac{\partial^2 u}{\partial \theta^2} + \kappa\frac{\partial^4 u}{\partial \theta^4} + (\beta_1 + \beta_2)u - \beta_2 w = 0, \tag{1b}$$

where $w(\theta, t)$ and $u(\theta, t)$ are deformations of the first and second rings, respectively, at a spatially fixed (i.e., not rotating) angular position θ, β_1 is the stiffness of the elastic foundation connecting a ring with the ground, β_2 is the stiffness of the elastic foundation coupling the two rings, and κ is the bending stiffness of each ring. For cases where $\kappa > 0$, both rings are dispersive media. When $\kappa = 0$, the rings are non-dispersive and can be regarded as strings. The parity symmetry operation exchanges the deformations of the two rings (or non-dispersive strings when $\kappa = 0$), i.e., $P\,[w(\theta, t), u(\theta, t)]^T = [u(\theta, t), w(\theta, t)]^T$. Based on Eq. (1), the system is PT symmetric regardless of whether the sub-units are dispersive or not. The Hamiltonian of the two counter-rotating rings is obtained by rewriting the equation of motion in Eq. (1) in the form of a Schrödinger equation $i\frac{\partial}{\partial t}\mathbf{q} = \mathbf{H}\mathbf{q}$, where $\mathbf{q} = (i\frac{\partial w}{\partial t}, w, i\frac{\partial u}{\partial t}, u)^T$. The Hamiltonian $\mathbf{H}$ is provided in the supplementary material, Note 2. As shown in supplementary material, Note 2, the Hamiltonian is invariant under the PT operation.

Substitution of $(w(\theta, t), u(\theta, t)) = \exp[i(\omega t + k\theta)](\phi_w, \phi_u)$ into Eq. (1) yields the eigenvalue problems for each nodal diameter k (angular wave number),

$$\begin{pmatrix} -\omega^2 + 2\Omega k\omega - (\Omega^2 - 1)k^2 + \kappa k^4 + \beta_1 + \beta_2 & -\beta_2 \\ -\beta_2 & -\omega^2 - 2\Omega k\omega - (\Omega^2 - 1)k^2 + \kappa k^4 + \beta_1 + \beta_2 \end{pmatrix}\begin{pmatrix} \phi_w \\ \phi_u \end{pmatrix} = 0. \tag{2}$$

Four eigenvalues are solved from Eq. (2) as

$$\omega_{1,2}^{+} = \pm\sqrt{(\Omega^2 + 1)k^2 + \kappa k^4 + \beta_1 + \beta_2 + \sqrt{\beta_2^2 + 4\Omega^2 k^2(\kappa k^4 + k^2 + \beta_1 + \beta_2)}},$$

$$\omega_{1,2}^{-} = \pm\sqrt{(\Omega^2 + 1)k^2 + \kappa k^4 + \beta_1 + \beta_2 - \sqrt{\beta_2^2 + 4\Omega^2 k^2(\kappa k^4 + k^2 + \beta_1 + \beta_2)}}. \tag{3}$$

The eigenvalues $\omega_{1,2}^{+}$ are always real-valued while $\omega_{1,2}^{-}$ are either real-valued or purely imaginary. When the eigenvalues $\omega_{1,2}^{-}$ are purely imaginary, divergence instability occurs. In this case, the amplitude of the associated k nodal diameter component associated with the negative imaginary eigenvalue grows exponentially with time. The exceptional points are the speeds Ω such that $\omega_{1,2}^{-} = 0$. Two exceptional points occur for each nodal diameter k,

$$\Omega_{E1} = \sqrt{1 + (\kappa k^4 + \beta_1)/k^2}, \tag{4a}$$

$$\Omega_{E2} = \sqrt{1 + (\kappa k^4 + \beta_1 + 2\beta_2)/k^2}. \tag{4b}$$

Figure 2 illustrates the loci of the eigenvalues $\omega_{1,2}^{-}$ for nodal diameter $k = 2$. The loci in Fig. 2(a) are for counter-rotating rings (dispersive) while those in Fig. 2(b) are for counter-rotating strings (non-dispersive). In both cases, the loci are divided into three phases (phases I, III, and V in Fig. 2) by two exceptional points (II and IV). The phases I and V are PT-exact phases where both of the eigenvalues are real, while phase III is a PT-broken phase where both eigenvalues are purely imaginary. A comparison between Figs. 2(a) and 2(b) demonstrates that the occurrence of exceptional points does not rely on the dispersive property of the sub-units.

The counter-rotating rings/strings have modal properties associated with the system symmetry. According to Eq. (3), the four eigenvalues for the nodal diameter k are identical to those for the nodal diameter $-k$. Therefore, each eigenvalue has double degeneracy away from the exceptional points. At the exceptional points, the eigenvalues $\omega_{1,2}^{-}$ coalesce into an eigenvalue with quadruple

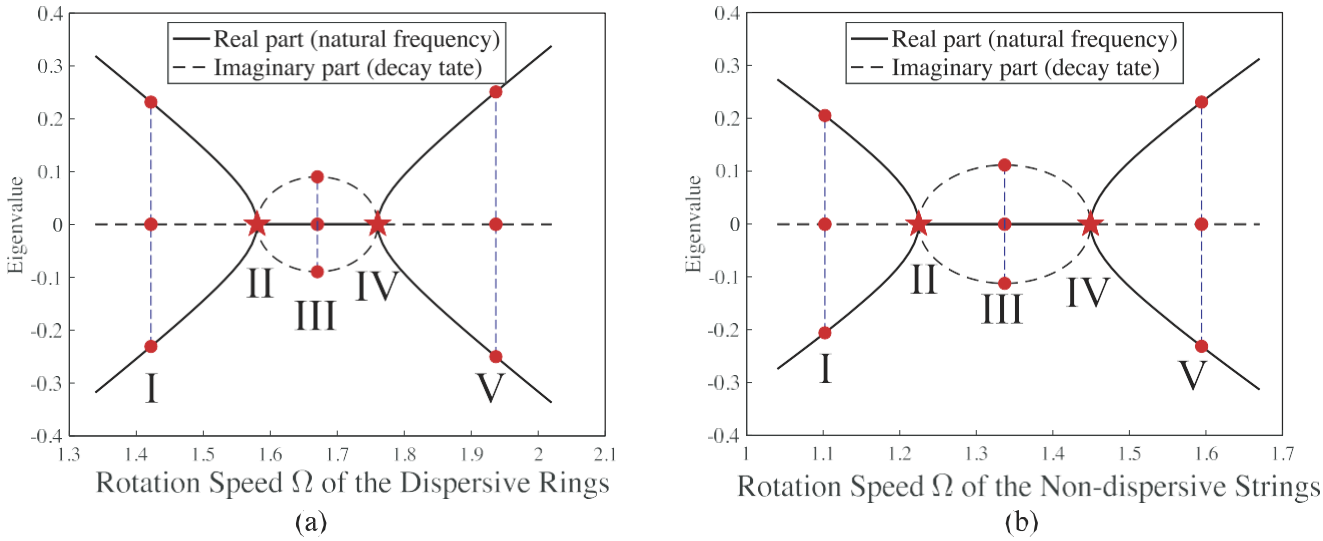

FIG. 2. Eigenvalues of PT symmetric counter-rotating (a) dispersive rings ($\kappa = 1$) and (b) non-dispersive strings ($\kappa = 0$). The solid lines represent the real parts of the eigenvalues, and the dashed lines represent the imaginary parts. Exceptional points are labeled by stars. The phases separated by the exceptional points are PT-exact phase (I), PT-broken phase (III), and PT-exact phase (V).

degeneracy. Based on the derivation in the supplementary material, Note 3, if $\exp(ik\theta)(\phi_w, \phi_u)^T$ is a vibration mode of the system associated with the eigenvalue ω, we have that

A. $\exp(ik\theta)P(\phi_w, \phi_u)^T = \exp(ik\theta)(\phi_u, \phi_w)^T$ is a mode associated with the eigenvalue $-\omega$,
B. $\exp(-ik\theta)P(\phi_w, \phi_u)^T = \exp(-ik\theta)(\bar{\phi}_u, \bar{\phi}_w)^T$ is a mode associated with the eigenvalue $\bar{\omega}$, and
C. $\exp(-ik\theta)(\phi_w, \phi_u)^T$ is a mode associated with the eigenvalue $-\omega$, where $\bar{\omega}$ is the complex conjugate of ω.

These modal properties explain why the phase with imaginary eigenvalues are in a PT-broken phase while others are in PT-exact phases. When ω is real, application of the PT operator on the mode $\exp(ik\theta)(\phi_w, \phi_u)^T$ gives $PT\exp(ik\theta)(\phi_w, \phi_u)^T = \exp(-ik\theta)(\phi_u, \phi_w)^T$, which is the mode associated with the eigenvalue $\bar{\omega}$. Because $\omega = \bar{\omega}$ when ω is real-valued, application of the PT operator on a mode yields a mode associated with the same eigenvalue. In other words, the subspace spanned by the eigenvectors associated with a real-valued eigenvalue is invariant under the PT operation. Therefore, the phases where the eigenvalues are real-valued are PT-exact phases. In contrast, when ω is purely imaginary, $\bar{\omega} = -\omega$. The PT symmetry operation maps the subspace spanned by the eigenvectors associated with ω to the subspace associated with $-\omega$. Therefore, the phase with purely imaginary eigenvalues is a PT-broken phase.

The counter-rotating rings/strings are analyzed in the PT-exact and PT-broken phases. To illustrate the deformation of the elastic continuum rings, we focus on the locations of maximum ring deformation as depicted in Fig. 1(b). The initial conditions for all the simulations in Fig. 3 consist of the deformations $u(\theta, 0) = \cos(2\theta)$ and $u(\theta, 0) = \cos(2\theta + \pi/3)$ with zero initial velocity. Only the modes with nodal diameter $k = 2$ and -2 are excited, so the two locations of maximum deformation on each ring form a diameter as shown in Fig. 1(b). For the cases in the PT-exact phases [(I) and (V) in Fig. 3(a)], the locations of maximum deformation are moving, as seen by a ground-based observer, because all the excited modes are associated with real-valued eigenvalues and are traveling waves. For the PT-broken phase [Fig. 3(a) (III)], the locations of maximum deformation on the two rings rotate monotonically to fixed (as seen by a ground-based observer) angular locations. The diameters of the locations of maximum deformation on the two rings finally converge to a fixed angle φ. The angle φ is proved to be a function of the rotating speed (see details in the supplementary material, Note 4). Similar phenomena occur for the cases at the exceptional points [(II) and (IV) in Fig. 3(a)], where the angle φ is 0 and $\pi/2$ for points (II) and (IV), respectively. The reason for the fixed locations of maximum deformation is that divergence instability occurs. In a PT-broken phase, the k nodal diameter modes associated with negative imaginary eigenvalues grow exponentially with time. These modes dominate the dynamic response as time passes. Because they are associated with imaginary eigenvalues, these dominant modal components do not propagate circumferentially. The initial locations of maximum deformation are determined by the initial deformations and move to fixed angular locations that are determined by the dominant modes. The cases at exceptional points can be explained similarly, except that the modes associated with the degenerate zero eigenvalues grow linearly, rather than exponentially, with time.

Dispersive properties of sub-units have no impact on the PT-symmetry-related dynamic properties of counter-rotating gyroscopic systems. A comparison between the subfigures in Fig. 3 demonstrates that the counter-rotating strings also experience two phase transitions across the exceptional points in Fig. 2(b). The behavior of the locations of maximum deformation in each of five

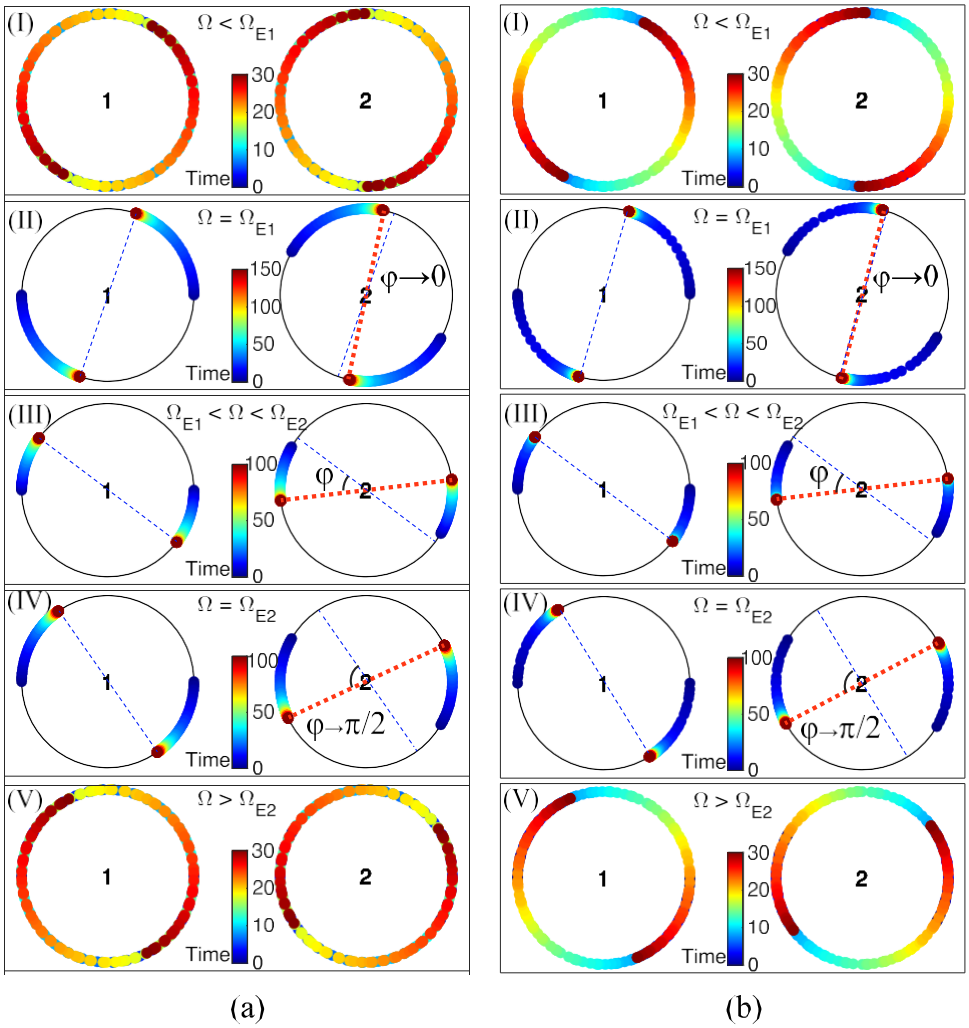

FIG. 3. Evolution of deformation profiles of PT symmetric counter-rotating (a) dispersive rings and (b) non-dispersive strings. Cases (I)–(V) correspond to the rotational speeds and eigenvalues in Fig. 2. The systems are in the PT-exact phases for cases (I) and (V), at exceptional points for cases (II) and (IV), and in the PT-broken phases for cases (III). For each case, we plot the trajectories of the locations of maximum deflection for both strings/rings, with markers colored according to the time.

scenarios (I)–(V) in Fig. 3 is qualitatively identical to those discussed above regardless of whether the sub-units are dispersive or not.

In conclusion, counter-rotating gyroscopic systems are proposed as an alternative design of PT symmetric systems to those relying on loss and gain units. We demonstrate that the PT symmetry and the occurrence of exceptional points in counter-rotating gyroscopic systems are independent of the dispersive properties of the sub-units. Spontaneous symmetry breaking across the exceptional points in counter-rotating gyroscopic systems results in transitions from system stability to instability or vice versa. In a gyroscopic system with two counter-rotating circular rings, the system dynamics experience a phase transition from a system with constantly propagating locations of maximum deformation to one with a fixed location of maximum deflection, despite the constant rotation speed of the rings. Counter-rotating gyroscopic systems provide a new platform for further studying PT-phase transition dynamics and related nonlinear dispersive physics in PT symmetric systems, including solitary waves and inelastic wave scattering.

See Note 1 of the supplementary material for derivation of the PT symmetric conditions for a general gyroscopic system, Note 2 for the Hamiltonian of two counter-rotating rings, Note 3 for modal properties of two counter-rotating rings, and Note 4 for the property of the angle between locations of maximum deformations on the two rings.

CS thanks the support from National Science Foundation under grant number CMMI-2037565.

AUTHOR DECLARATIONS

Conflict of Interest

The authors declare no conflicts of interest for this research.

DATA AVAILABILITY

Data sharing is not applicable to this article as no new data were created or analyzed in this study.

REFERENCES

[1]C. M. Bender and S. Boettcher, Phys. Rev. Lett. **80**, 5243 (1998).
[2]W. D. Heiss, J. Phys. A: Math. Gen. **37**, 2455 (2004).
[3]C. M. Bender, Rep. Prog. Phys. **70**, 947 (2007).
[4]M.-A. Miri and A. Alù, Science **363**, eaar7709 (2019).
[5]R. El-Ganainy, K. G. Makris, M. Khajavikhan, Z. H. Musslimani, S. Rotter, and D. N. Christodoulides, Nat. Phys. **14**, 11 (2018).
[6]N. Bender, S. Factor, J. D. Bodyfelt, H. Ramezani, D. N. Christodoulides, F. M. Ellis, and T. Kottos, Phys. Rev. Lett. **110**, 234101 (2013).
[7]J. Schindler, Z. Lin, J. M. Lee, H. Ramezani, F. M. Ellis, and T. Kottos, J. Phys. A: Math. Theor. **45**, 444029 (2012).
[8]Y. Li, Y.-G. Peng, L. Han, M.-A. Miri, W. Li, M. Xiao, X.-F. Zhu, J. Zhao, A. Alù, S. Fan, and C.-W. Qiu, Science **364**, 170 (2019).
[9]B. Peng, S¸. K. Özdemir, F. Lei, F. Monifi, M. Gianfreda, G. L. Long, S. Fan, F. Nori, C. M. Bender, and L. Yang, Nat. Phys. **10**, 394 (2014).
[10]C. E. Rüter, K. G. Makris, R. El-Ganainy, D. N. Christodoulides, M. Segev, and D. Kip, Nat. Phys. **6**, 192 (2010).
[11]A. Regensburger, C. Bersch, M.-A. Miri, G. Onishchukov, D. N. Christodoulides, and U. Peschel, Nature **488**, 167 (2012).
[12]X. Zhu, L. Feng, P. Zhang, X. Yin, and X. Zhang, Opt. Lett. **38**, 2821 (2013).
[13]R. Fleury, D. L. Sounas, and A. Alù, Phys. Rev. Lett. **113**, 023903 (2014).
[14]X. Zhu, H. Ramezani, C. Shi, J. Zhu, and X. Zhang, Phys. Rev. X **4**, 031042 (2014).
[15]R. Fleury, D. Sounas, and A. Alù, Nat. Commun. **6**, 5905 (2015).
[16]C. Shi, M. Dubois, Y. Chen, L. Cheng, H. Ramezani, Y. Wang, and X. Zhang, Nat. Commun. **7**, 11110 (2016).
[17]W. Zhu, X. Fang, D. Li, Y. Sun, Y. Li, Y. Jing, and H. Chen, Phys. Rev. Lett. **121**, 124501 (2018).
[18]S. R. Craig, P. J. Welch, and C. Shi, Appl. Phys. Lett. **115**, 051903 (2019).
[19]H. Hodaei, A. U. Hassan, S. Wittek, H. Garcia-Gracia, R. El-Ganainy, D. N. Christodoulides, and M. Khajavikhan, Nature **548**, 187 (2017).
[20]Z. Dong, Z. Li, F. Yang, C.-W. Qiu, and J. S. Ho, Nat. Electron. **2**, 335 (2019).
[21]H. Zhang, R. Huang, S.-D. Zhang, Y. Li, C.-W. Qiu, F. Nori, and H. Jing, Nano Lett. **20**, 7594 (2020).
[22]S. Longhi, Phys. Rev. A **82**, 031801 (2010).
[23]Y. D. Chong, L. Ge, and A. D. Stone, Phys. Rev. Lett. **106**, 093902 (2011).
[24]B. Peng, S¸. K. Özdemir, S. Rotter, H. Yilmaz, M. Liertzer, F. Monifi, C. M. Bender, F. Nori, and L. Yang, Science **346**, 328 (2014).
[25]Z. J. Wong, Y.-L. Xu, J. Kim, K. O'Brien, Y. Wang, L. Feng, and X. Zhang, Nat. Photonics **10**, 796 (2016).
[26]J.-W. Ryu, S.-Y. Lee, and S. W. Kim, Phys. Rev. A **79**, 053858 (2009).
[27]H. Ramezani, T. Kottos, R. El-Ganainy, and D. N. Christodoulides, Phys. Rev. A **82**, 043803 (2010).
[28]Z. Lin, H. Ramezani, T. Eichelkraut, T. Kottos, H. Cao, and D. N. Christodoulides, Phys. Rev. Lett. **106**, 213901 (2011).
[29]L. Ge, Y. D. Chong, and A. D. Stone, Phys. Rev. A **85**, 023802 (2012).
[30]L. Meirovitch, AIAA J. **12**, 1337 (1974).
[31]L. Meirovitch, *Principles and Techniques of Vibrations* (Prentice-Hall, Inc., Upper Saddle River, NJ, 1997), p. 07458.
[32]R. G. Parker, ASME J. Appl. Mech. **65**, 134 (1998).
[33]R. G. Parker, J. Sound Vib. **221**, 205 (1999).
[34]K. Y. Bliokh, Y. Gorodetski, V. Kleiner, and E. Hasman, Phys. Rev. Lett. **101**, 030404 (2008).
[35]K. Y. Bliokh, F. J. Rodríguez-Fortuño, F. Nori, and A. V. Zayats, Nat. Photonics **9**, 796 (2015).
[36]A. Aiello, P. Banzer, M. Neugebauer, and G. Leuchs, Nat. Photonics **9**, 789 (2015).
[37]C. Shi, R. Zhao, Y. Long, S. Yang, Y. Wang, H. Chen, J. Ren, and X. Zhang, Natl. Sci. Rev. **6**, 707 (2019).
[38]L. Lu, J. D. Joannopoulos, and M. Soljac˘ic´, Nat. Photonics **8**, 821 (2014).
[39]Z. Yang, F. Gao, X. Shi, X. Lin, Z. Gao, Y. Chong, and B. Zhang, Phys. Rev. Lett. **114**, 114301 (2015).
[40]P. Lodahl, S. Mahmoodian, S. Stobbe, A. Rauschenbeutel, P. Schneeweiss, J. Volz, H. Pichler, and P. Zoller, Nature **541**, 473 (2017).